Published in final edited form as:
Hum Mutat. 2009 January ; 30(1): 61–68. doi:10.1002/humu.20814.

A Balanced Chromosomal Translocation Disrupting *ARHGEF9* Is Associated With Epilepsy, Anxiety, Aggression, and Mental Retardation

Vera M. Kalscheuer[1,*], **Luciana Musante**[1], **Cheng Fang**[2], **Kirsten Hoffmann**[1], **Celine Fuchs**[3], **Eloisa Carta**[3], **Emma Deas**[3], **Kanamarlapudi Venkateswarlu**[4], **Corinna Menzel**[1], **Reinhard Ullmann**[1], **Niels Tommerup**[5], **Leda Dalprà**[6], **Andreas Tzschach**[1], **Angelo Selicorni**[7], **Bernhard Lüscher**[2], **Hans-Hilger Ropers**[1], **Kirsten Harvey**[3], and **Robert J. Harvey**[3,*]

[1]Department of Human Molecular Genetics, Max Planck Institute for Molecular Genetics, Berlin, Germany

[2]Department of Biochemistry and Molecular Biology and Penn State Neuroscience Institute, Penn State University, University Park, Pennsylvania, USA

[3]Department of Pharmacology, The School of Pharmacy, London, United Kingdom

[4]Institute of Life Science, School of Medicine, Swansea University, Swansea, United Kingdom

[5]Department of Cellular and Molecular Medicine, Wilhelm Johannsen Centre for Functional Genome Research, Copenhagen, Denmark

[6]Department of Neurosciences and Biomedical Technologies, University of Milan-Bicocca, Monza, Italy

[7]Department of Pediatrics, Istituti di Ricovero e Cura a Carattere Scientifico (IRCCS) Policlinico Foundation, Milan, Italy

Abstract

Clustering of inhibitory γ-aminobutyric acid$_A$ (GABA$_A$) and glycine receptors at synapses is thought to involve key interactions between the receptors, a “scaffolding” protein known as gephyrin and the RhoGEF collybistin. We report the identification of a balanced chromosomal translocation in a female patient presenting with a disturbed sleep-wake cycle, late-onset epileptic seizures, increased anxiety, aggressive behavior, and mental retardation, but not hyperekplexia. Fine mapping of the breakpoint indicates disruption of the collybistin gene (ARHGEF9) on chromosome Xq11, while the other breakpoint lies in a region of 18q11 that lacks any known or predicted genes. We show that defective collybistin transcripts are synthesized and exons 7–10 are replaced by cryptic exons from chromosomes X and 18. These mRNAs no longer encode the pleckstrin homology (PH) domain of collybistin, which we now show binds phosphatidylinositol-3-phosphate (PI3P/ PtdIns-3-P), a phosphoinositide with an emerging role in membrane trafficking and signal transduction, rather than phosphatidylinositol 3,4,5-trisphosphate

[*]Correspondence to: Robert J. Harvey, Department of Pharmacology, The School of Pharmacy, London WC1N 1AX, United Kingdom. robert.harvey@pharmacy.ac.uk. [*]Correspondence to: Vera M. Kalscheuer, Department of Human Molecular Genetics, Max Plank Institute for Molecular Genetics, Ihnestrasse 73, D-14195 Berlin, Germany. kalscheu@molgen.mpg.de.
Present affiliation for Cheng Fang: Oregon Health and Science University, Portland, Oregon. Present affiliation for Emma Deas: Department of Molecular Neuroscience, Institute of Neurology, London, United Kingdom.
Requests for materials (subject to a Material Transfer Agreement) should be addressed to V.M.K. (kalscheu@molgen.mpg.de) or R.J.H. (robert.harvey@pharmacy. ac.uk).

The Supplementary Material referred to in this article can be accessed at http://www.interscience.wiley.com/jpages/1059-7794/suppmat.

(PIP3/PtdIns-3,4,5-P) as previously suggested in the “membrane activation model” of gephyrin clustering. Consistent with this finding, expression of truncated collybistin proteins in cultured neurons interferes with synaptic localization of endogenous gephyrin and $GABA_A$ receptors. These results suggest that collybistin has a key role in membrane trafficking of gephyrin and selected $GABA_A$ receptor subtypes involved in epilepsy, anxiety, aggression, insomnia, and learning and memory.

Keywords

$GABA_A$ receptors; glycine receptors; collybistin; *ARHGEF9*; gephyrin; clustering; anxiety; epilepsy; mental retardation; aggression

Introduction

Inhibitory γ-aminobutyric $acid_A$ ($GABA_A$) and glycine receptors are heteropentameric ligand-gated chloride ion channels that usually facilitate fast-response, inhibitory neurotransmission in the human brain and spinal cord. Defects in mammalian glycinergic neurotransmission result in a complex motor disorder characterized by neonatal hypertonia and an exaggerated startle reflex, known as hyperekplexia. In humans, missense and nonsense mutations in the GlyR α1 gene (*GLRA1*; MIM# 138491) and the glycine transporter GlyT2 (*SLC6A5*; MIM# 604159) are the major causes of this disorder [Shiang et al., 1993; Rees et al., 2006]. By contrast, mutations in $GABA_A$ receptor ($GABA_AR$) subunit genes are associated with rare familial forms of idiopathic generalized epilepsy (IGE), such as childhood absence epilepsy (CAE), generalized epilepsy with generalized seizures plus (GEFS+), and juvenile myoclonic epilepsy (JME). However, despite the multiple subunits available for assembly of heteropentameric receptors (α1–6, β1–3, γ1–3, δ, ε, θ, and π) to date, surprisingly few mutations linked to IGEs have been identified in $GABA_AR$ subunit genes. Missense or frameshift mutations in the $GABA_AR$ α1 subunit gene (*GABRA1*; MIM# 137160) are associated with JME [Cossette et al., 2002] and CAE [Maljevic et al., 2006]. By contrast, missense, splice-site mutations, and deletions in *GABRG2* (MIM# 137164), encoding the γ2 subunit, were found in families with GEFS+ and CAE with febrile seizures [Baulac et al., 2001; Wallace et al., 2001; Harkin et al., 2002; Kananura et al., 2002; Audenaert et al., 2006]. Consistent with this finding, γ2 subunit missense mutations appear to cause temperature-dependent $GABA_AR$ trafficking deficiencies [Kang et al., 2006]. The limited contribution of $GABA_AR$ subunit gene mutations to epilepsy may reflect the different spatial and temporal expression patterns and biological roles of specific $GABA_AR$ subtypes, functional redundancy via gene compensation, and the considerable genetic heterogeneity found in IGEs [Heron et al., 2007]. However, we consider that aberrant trafficking or defective synaptic localization of GlyR and/or $GABA_ARs$ could also have a significant impact in both hyperekplexia and epilepsy. Several lines of evidence suggest that synaptic localization of GlyRs and some $GABA_ARs$ is critically dependent on interaction of these receptors with a “scaffolding” protein known as gephyrin, which is in turn targeted to synapses by collybistin/hPEM2 [Kins et al., 2000; Kneussel and Betz, 2000; Harvey et al., 2004], a GDP-GTP exchange factor [Xiang et al., 2006] for the GTPase Cdc42. We report here a balanced chromosomal translocation affecting the collybistin gene (*ARHGEF9*; MIM# 300429) in a patient with a disturbed sleep-wake cycle, epilepsy, increased anxiety, aggressive behavior, and mental retardation, but not hyperekplexia, suggesting a broad disruption of several GABAergic but not glycinergic circuits.

Materials and Methods

Mapping the Balanced Chromosomal Translocation in *ARHGEF9*

Patient and control samples were obtained with informed consent. Karyotype analysis was performed using standard high-resolution techniques. For breakpoint mapping, YACs, BACs, and PACs were prepared by standard techniques, labeled with appropriately coupled dUTPs by nick translation or directly labeled by Degenerate Oligonucleotide Primer PCR (DOP-PCR), and used as probes for fluorescence in situ hybridization (FISH) as described [Wirth et al., 1999]. For Southern blotting, PCR-amplified DNA probes were labeled with α[^{32}P]dCTP using random hexamers and hybridization buffer containing 10% (w/v) PEG 6000, 0.125 M Na_3PO_4, 0.25 M NaCl, 0.001 M EDTA, 7% (w/v) SDS, supplemented with salmon or herring sperm DNA. The probe used for breakpoint identification was amplified with primers ChrX-180019 and ChrX-181201. Suppression PCR on *Rsa*I-digested patient DNA was performed as described [Siebert et al., 1995] with adapter primer AP1 and chromosome X sequence-specific primer ChrX-180618, followed by a nested PCR with adapter primer AP2 and ChrX-180659. For breakpoint analysis of derivative chromosome 18, genomic patient DNA was amplified with primers Chr18-85079F1 and ChrX-181201. Sequences of all primers used in this study are provided in Supplementary Table S1 (available online at http://www.interscience.wiley.com/jpages/1059-7794/suppmat).

RT-PCR and 3′ RACE Analysis of *ARHGEF9* Transcripts

Total RNA was isolated from patient and control lymphoblastoid cell line using Trizol (Invitrogen, Carlsbad, CA) according to the manufacturer's recommendations. A total of 5 μg of RNA were used for reverse transcription with Superscript III (Invitrogen) in the presence of RNAguard (GE Healthcare, Chalfont, UK), using either oligonucleotide dT or random hexamers for priming. 3′ RACE was performed using primers hPEM2-Ex5 and hPEM2-Ex6 using the GeneRacer kit (Invitrogen) according to the manufacturer's directions. Full-length cDNAs were amplified using *Pfx* proofreading DNA polymerase (Invitrogen), using primers based on the human *ARHGEF9* cDNA sequence (NM_015185.2) and/or 3′ RACE fragments, cloned into the *Bam*HI and *Eco*RI sites of pRK5-myc and fully sequenced. All PCR products and cDNA clones were sequenced using BigDye terminator mix (Applied Biosystems, Warrington, UK) using an ABI 3100 (Applied Biosystems, Warrington, United Kingdom).

Gephyrin Clustering Assays in Cellular Models

Gephyrin clustering assays in cellular models were performed as previously described [Harvey et al., 2004]. HEK293 cells were cotransfected with pRK5myc-hPEM2 constructs at a 1:1 ratio with enhanced green fluorescent protein (pEGFP)-gephyrin using Effectine (Qiagen, Crawley, UK) and after 24 hrs in culture were fixed in 4% (w/v) PFA in PBS and immunostained with a 1:1,000 dilution of mouse anti-myc antibody (R950-25; Invitrogen), detected using a 1:500 dilution of AlexaFluor 488 goat anti-mouse secondary antibody (Invitrogen) and counterstained with a 1:10,000 dilution of ToPro-3 (T3605; Invitrogen).

Lipid Protein Overlay Assays

Lipid protein overlay assays were performed according to the method of Dowler et al. [2000]. Phosphoinositides (Cell Signals, Columbus, OH) were dissolved in methanol/chloroform/water (2:1:0.8) to give concentrations in the range of 100–1.6 pmol/μl and spotted onto nitrocellulose filters (GE Healthcare, Chalfont, UK) and dried for 1 hr at room temperature (RT). Membranes were then blocked in Tris-buffered saline Tween-20 (TBST) (50 mM Tris-HCl pH 7.4, 150 mM NaCl, and 0.1% (v/v) Tween-20) containing 5% (w/v) skim milk powder for 1 hr at RT. Glutathione-S-transferase (GST)-tagged hPEM2 or

centaurin α1 were isolated from *E. coli* BL21 (DE3) from corresponding constructs cloned in pGEX4 T. GST-hPEM2 or GST-centaurin α1 (2 μg/ml) was then added to the blocking solution and incubated overnight at 4°C. The membranes were then washed three times with TBST. Bound protein was detected by immunoblotting with a 1:2,000 dilution of an anti-GST goat polyclonal antibody (27-4577-01; GE Healthcare) for 1 hr, three washes in TBST, and detected with a 1:2,500 dilution of horseradish peroxidase (HRP)-conjugated anti-goat immunoglobulin G (IgG) (A5420; Sigma-Aldrich, Gillingham, UK) for 1 hr, followed by three washes in TBST. HRP activity was detected using enhanced chemiluminescence reagent (ECL; GE Healthcare) and by exposing to X-ray film for 1 to 5 min.

Neuronal Cell Culture, Transfection, and Quantification of Gephyrin/$GABA_AR$ Clustering

Cultures of cortical neurons were generated from embryonic day 14.5 (E14.5) mouse embryos, as described previously [Essrich et al., 1998; Harvey et al., 2004]. They were transfected at 18 days in vitro (DIV) and processed for immunofluorescence analysis under permeabilized conditions 2 days later. The following primary antibodies were used: guinea pig anti-γ2 (1:1,500; a gift from J.M. Fritschy, University of Zurich, Switzerland), rabbit anti-myc (1:1,000, clone 9E10, generated in-house), and anti-gephyrin monoclonal antibody 7a (mAb7a) (1:1,000; a gift from H. Betz, Max-Planck-Institut für Hirnforschung, Frankfurt, Germany). Antibodies were detected with 1:500 dilutions of Alexa Fluor 488-conjugated goat anti-mouse, Cy3-conjugated donkey anti-guinea pig (Jackson ImmunoResearch, West Grove, PA), and Alexa Fluor 647 goat anti-rabbit (Invitrogen). Fluorescent images were captured from a Zeiss Axiophot 2 microscope (Carl Zeiss MicroImaging, Thornwood, NY) equipped with a 40 × 1.3 numerical aperture objective and an ORCA-100 video camera (Hamamatsu Photonics, Bridgewater, NJ) linked to an OpenLab imaging system (Improvision, Lexington, MA). Images were adjusted for contrast using OpenLab or FlowView software, respectively, and assembled into figure palettes using Adobe PhotoShop (Adobe Systems, San Jose, CA). For semiquantitative analyses of labeled $GABA_AR$ and gephyrin clusters, digitized microscopic images were recorded, and two dendritic segments of length 40 μm each were selected from each transfected neuron from three or more independent experiments [Harvey et al., 2004]. Immunoreactive puncta were automatically selected using OpenLab, applying a fluorescence intensity threshold corresponding to twice the diffuse fluorescence measured on the shaft of the same dendrite and a target size range of 0.2 to 2 μm in diameter. Statistical comparisons were performed using Student's *t*-test.

Results

The proband was the first child of healthy unrelated parents delivered at term via Cesarean section due to obstetric problems. Birth weight (3,140 g, 50th percentile) and length (50 cm, 50th percentile) were normal. At the age of 7 months, generalized hypotonia and psychomotor developmental arrest were noted. Cerebral nuclear magnetic resonance (NMR) results were normal and screening for inborn errors of metabolism excluded amino acid pathologies or organic acidurias. At the age of 1 year and 9 months her weight was 9.6 kg (5th percentile), height 75.5 cm (<5th percentile), and head circumference 46.9 cm (10th percentile). She was hypotonic and unable to sit without support. The EEG at this stage and 2 years later showed relatively slow rhythm and partial disorganization of basic activity. At the age of 6 years, her weight was 14 kg (<3rd percentile), height 98 cm (<3rd percentile), and head circumference 50 cm (25th–50th percentile). Dysmorphic features included a long and narrow face, high narrow palate, hypertrophy of the alveolar ridge, irregular teeth, and micrognathia (Fig. 1A). Although the patient was able to walk autonomously, she was hyperactive and had no verbal communication. At the age of 7 years, she developed generalized tonic-clonic seizures, which occurred during the initial sleeping phase, although

MRI scans were normal. Since the age of 8 years, the patient has suffered from frequent mood changes and a disturbed sleep-wake rhythm. She dislikes being touched by others or the proximity of other children. In situations where she becomes agitated, which can be triggered by changes in her environment, she shows self-injurious behaviors such as hand biting and punching her head. Likewise, she shows injurious behaviors against others. At the age of 12 years the patient was profoundly mentally retarded with a psychoeducational level of 7–12 months old. At the age of 14 years the parents noticed obstructive sleep apnea, which was treated by surgery. At a recent examination, at the age of 15 years her weight was 27 kg (≪3rd percentile), her height 140 cm (≪3rd percentile), and her occipital-frontal circumference was 53.5 cm (≪3rd percentile). She had few words or social responses and a reduced sensitivity to thermal pain was noted. Seizures, mood, and behavior problems improved through treatment with the benzodiazepine clonaze-pam, the GABA transaminase inhibitor valproic acid, and the atypical antipsychotic risperidone.

Karyotyping in this individual revealed a de novo balanced chromosomal translocation 46,X,t(X;18) (q11.1;q11.21), depicted in Figure 1B. Breakpoints were mapped by sequential FISH of genomic clones from both chromosomes 18 and X. On chromosome 18, the breakpoint lies within the genomic region of clones RP11-29E21 and RP11-885L22 (chr18: 24,344,568–24,564,620) (Fig. 1C, right panel), which does not contain any known or predicted genes. However, on chromosome X, we noted that BAC clone RP11-943J20, containing *ARHGEF9*, spanned the breakpoint (Fig. 1C, left panel). The breakpoint was localized by Southern blot analysis of patient DNA, which revealed aberrant patient-specific DNA fragments in several digests (Fig. 1D). Subsequent cloning and sequence analysis of the junctional fragment revealed that the breakpoint lies between exons 6 and 7 of *ARHGEF9* (Fig. 1E and F). We ruled out a deletion at the breakpoint on derivative chromosome 18 by sequencing the PCR-amplified breakpoint region (Fig. 1F), indicating that the translocation is balanced. Additional aberrations unrelated to this breakpoint were also excluded by array comparative genomic hybridization (CGH) analysis (Supplementary Fig. S1).

Since in balanced X-autosome translocations, the normal X chromosome is often preferentially inactivated [Kalz-Füller et al., 1999], RNA derived from an immortalized patient leukocyte cell line was tested for *ARHGEF9* transcripts. RT-PCR amplifications with primers located in *ARHGEF9* exons 5 and 7, which flank the breakpoint and in exons 8 and 10, which are both located proximal to the breakpoint on the derivative X chromosome, indicated that full-length *ARHGEF9* transcripts are absent in the patient, whereas products of the expected size were easily amplifiable from control RNA (Fig. 1G). This analysis verified that the chromosomal rearrangement has led to inactivation of the normal X chromosome and that *ARHGEF9* is subject to X inactivation. However, PCR products corresponding to exons 4–6 and exons 5–6, which in the patient are present on the derivative chromosome 18, indicated that truncated *ARHGEF9* transcripts are produced. Further analysis using 3′ RACE revealed two classes of *ARHGEF9* transcript containing exons 1–6 followed by cryptic exons derived from intronic or intergenic sequences on chromosomes X and 18, each containing a consensus polyadenylation signal (Fig. 2A; Supplementary Fig. S2). As a result, patient-specific truncated *ARHGEF9* mRNAs are generated, producing two classes of truncated proteins designated hPEM-X and hPEM-18. Interestingly, splicing of these cryptic exons results in the loss of the collybistin pleckstrin homology (PH) domain and C-terminus. Using immobilized phosphoinositides and purified GST-collybistin in overlay assays [Dowler et al., 2000], we determined that the PH domain is required for collybistin function (Fig. 2C) since it binds the phosphoinositide PI3P (PtdIns-3-P/ phosphatidylinositol-3-phosphate), a phosphoinositide with an emerging role in membrane trafficking and signal transduction [Falasca and Maffucci, 2006]. This result was somewhat unexpected, since collybistin has previously been suggested to bind phosphatidylinositol

3,4,5-trisphosphate (PIP3/PtdIns-3,4,5-P) in the "membrane activation model" of gephyrin clustering [Kneussel and Betz, 2000]. However, controls using centaurin α1, a known PIP2 and PIP3 binding protein [Venkateswarlu et al., 2004], verified that our overlay assays were capable of detecting binding to these phosphoinositides (Fig. 2C).

Western blot analysis of myc-tagged hPEM constructs expressed in HEK293 cells indicates that the aberrant hPEM2-18 and hPEM2-X proteins are stable and expressed at levels equivalent to $hPEM2_{SH3+}$ and $hPEM2_{SH3-}$ when normalized to endogenous α-tubulin (Fig. 3A and B). Coexpression of myc-tagged hPEM2 proteins with EGFP-gephyrin in HEK293 cells revealed that, as expected [Kins et al., 2000; Harvey et al., 2004], variants containing the regulatory SH3 domain ($hPEM2_{SH3+}$) colocalize with EGFP-gephyrin in large intracellular aggregates (Fig. 3C), while $hPEM2_{SH3-}$, lacking the SH3 domain, directs EGFP-gephyrin to submembrane clusters (Fig. 3D). However, although hPEM2-18 (Fig. 3E) and hPEM2-X (Fig. 3F) lack the SH3 domain, these proteins colocalize with EGFP-gephyrin and do not direct the formation of submembrane microaggregates. To examine the effects of these proteins on neuronal gephyrin and $GABA_AR$ γ2 subunit clustering, we expressed these hPEM2 constructs in primary cultures of mouse cortical neurons. Punctate immunofluorescent staining for these proteins is representative of postsynaptic $GABA_AR$ and gephyrin clusters, respectively. Overexpression of myc-$hPEM2_{SH3+}$ or myc-$hPEM2_{SH3-}$ did not interfere with the colocalization of gephyrin or $GABA_ARs$ in synaptic clusters (Fig. 4A–D). Quantitative analysis revealed that neither $hPEM2_{SH3+}$ nor myc-$hPEM2_{SH3-}$ influence gephyrin puncta number (Fig. 4I) although deletion of the regulatory SH3 domain caused a modest increase in puncta size (Fig. 4J). By contrast, in neurons expressing myc-hPEM2-X (Fig. 4E, F) and myc-hPEM2-18 (Fig. 4G and H), punctuate gephyrin and $GABA_AR$ immunoreactivity was significantly reduced, suggesting that these truncated proteins can act in a dominant-negative manner and interfere with the accumulation of endogenous gephyrin and $GABA_ARs$ at synaptic sites. Quantitative analyses of the punctuate gephyrin immunofluorescence (Fig. 4I and J) confirmed that the number of gephyrin clusters was dramatically reduced, along with a significant reduction in size of the few remaining clusters.

Discussion

We describe a balanced chromosomal translocation truncating *ARHGEF9* that results in a range of clinical symptoms including a disturbed sleep-wake cycle, late-onset epileptic seizures, increased anxiety, aggressive behavior, and mental retardation. The translocation results in the production of functionally defective collybistin isoforms, lacking the PH domain and C-terminus. Loss of the collybistin PH domain is predicted to abolish PI3P binding, but does not affect interactions with gephyrin via the RhoGEF domain. We demonstrate that these truncated collybistin isoforms cause loss of synaptic gephyrin and $GABA_ARs$ via a dominant-negative mechanism, suggesting that the loss of specific $GABA_AR$ subtypes may underlie the symptoms observed in this individual. For example, mutations in human $GABA_AR$ α1 and γ2 subunit genes are associated with various types of IGEs [Baulac et al., 2001; Wallace et al., 2001; Cossette et al., 2002; Harkin et al., 2002; Kananura et al., 2002; Audenaert et al., 2006; Maljevic et al., 2006], while a mutation in the $GABA_AR$ β3 subunit gene (*GABRB3*) was reported in an individual with chronic insomnia [Buhr et al., 2002]. Homozygous $GABA_AR$ γ2 subunit knockout mice show retarded growth, sensorimotor dysfunction, a reduced life-span, and epileptic seizures [Günther et al., 1995; Essrich et al., 1998; Schweizer et al., 2003], while mice heterozygous for γ2 exhibit enhanced anxiety and a memory bias for threat cues, resulting in heightened sensitivity to negative associations [Crestani et al., 1999]. This may be linked to $GABA_ARs$ containing the α2 subunit, which are responsible for the anxiolytic effects of benzodiazepines [Löw et al., 2000]. By contrast, a loss of $GABA_ARs$ containing the α3 subunit induces a

hyperdopaminergic phenotype involving a deficit in sensorimotor gating [Yee et al., 2005], a common feature among psychiatric conditions, including schizophrenia. In this regard, it is noteworthy that the individual in this study responded to the use of antipsychotics and mood stabilizing drugs.

In conclusion, it is now apparent that different mutations in *ARHGEF9* give rise to a diverse range of clinical symptoms (Table 1). The missense mutation p.G55A in the SH3 domain gives rise to a severe phenotype encompassing hyperekplexia, drug-resistant seizures, and premature death, caused by somatic and dendritic trapping of gephyrin and receptors by collybistin aggregates [Harvey et al., 2004]. By contrast, a female patient with an X chromosome inversion affecting one copy of *ARHGEF9*, but with low expression from the unaffected *ARHGEF9* copy, suffered from mild mental retardation and sensory hyperarousal, but not seizures or hyperekplexia [Marco et al., 2008]. Thus, comparatively severe phenotypes are observed when dominant-negative forms of hPEM2 are expressed, as previously shown for the p.G55A mutation [Harvey et al., 2004] and the translocation reported here, which sequester gephyrin and $GABA_A$Rs from synaptic sites. Collybistin may also be dispensable for GlyR clustering, since hyperekplexia does not appear to be a common feature in humans with *ARHGEF9* rearrangements, nor collybistin knockout mice [Papadopoulos et al., 2007], which show increased levels of anxiety and impaired spatial learning due to a selective loss of $GABA_A$Rs in the hippocampus and the basolateral amygdala. This suggests that additional RhoGEFs involved in inhibitory receptor clustering remain to be identified.

Supplementary Material

Refer to Web version on PubMed Central for supplementary material.

Acknowledgments

We are grateful to the patient and her family. We thank D. Singh for initial help with RT-PCR experiments and S. Kübart, U. Fischer, H. Freier, and H. Madle for excellent technical existence. We thank Jean-Marc Fritschy (University of Zurich, Switzerland) and Heinrich Betz (Max-Planck Institut für Hirnforschung, Frankfurt, Germany) for generous gifts of $GABA_A$R γ2 subunit and gephyrin antibodies, respectively. This work was supported by the Medical Research Council (G0500833 and G0601585 to R.J.H.; G0501258 to K.H.; and G0401232 to V.K.), the Biotechnology and Biological Sciences Research Council (BB/C515455/1 to V.K.), the Deutsche Forschungsgemeinshaft (SFB577 to V.M.K. and H.H.R.), and the National Institute of Mental Health (MH60989 and MH60989 to B.L.). The Wilhelm Johannsen Centre for Functional Genome Research is supported by the Danish National Research Foundation.

References

Audenaert D, Schwartz E, Claeys KG, Claes L, Deprez L, Suls A, Van Dyck T, Lagae L, Van Broeckhoven C, Macdonald RL, De Jonghe P. A novel GABRG2 mutation associated with febrile seizures. Neurology. 2006; 67:687–690. [PubMed: 16924025]

Baulac S, Huberfeld G, Gourfinkel-An I, Mitropoulou G, Beranger A, Prud'homme JF, Baulac M, Brice A, Bruzzone R, LeGuern E. First genetic evidence of $GABA_A$ receptor dysfunction in epilepsy: a mutation in the γ2-subunit gene. Nat Genet. 2001; 28:46–48. [PubMed: 11326274]

Buhr A, Bianchi MT, Baur R, Courtet P, Pignay V, Boulenger JP, Gallati S, Hinkle DJ, Macdonald RL, Sigel E. Functional characterization of the new human $GABA_A$ receptor mutation $\beta 3^{R192\ H}$. Hum Genet. 2002; 111:154–160. [PubMed: 12189488]

Cossette P, Liu L, Brisebois K, Dong H, Lortie A, Vanasse M, Saint-Hilaire JM, Carmant L, Verner A, Lu WY, Wang YT, Rouleau GA. Mutation of GABRA1 in an autosomal dominant form of juvenile myoclonic epilepsy. Nat Genet. 2002; 31:184–189. [PubMed: 11992121]

Crestani F, Lorez M, Baer K, Essrich C, Benke D, Laurent JP, Belzung C, Fritschy JM, Lüscher B, Möhler H. Decreased $GABA_A$-receptor clustering results in enhanced anxiety and a bias for threat cues. Nat Neurosci. 1999; 2:833–839. [PubMed: 10461223]

Dowler S, Currie RA, Campbell DG, Deak M, Kular G, Downes CP, Alessi DR. Identification of pleckstrin-homology-domain-containing proteins with novel phosphoinositide-binding specificities. Biochem J. 2000; 351:19–31. [PubMed: 11001876]

Essrich C, Lorez M, Benson JA, Fritschy JM, Lüscher B. Postsynaptic clustering of major $GABA_A$ receptor subtypes requires the γ2 subunit and gephyrin. Nat Neurosci. 1998; 1:563–571. [PubMed: 10196563]

Falasca M, Maffucci T. Emerging roles of phosphatidylinositol 3-monophosphate as a dynamic lipid second messenger. Arch Physiol Biochem. 2006; 112:274–284. [PubMed: 17178602]

Günther U, Benson J, Benke D, Fritschy JM, Reyes G, Knoflach F, Crestani F, Aguzzi A, Arigoni M, Lang Y, Bluethmann H, Möhler H, Lüscher B. Benzodiazepine-insensitive mice generated by targeted disruption of the γ2 subunit gene of γ-aminobutyric acid type A receptors. Proc Natl Acad Sci USA. 1995; 92:7749–7753. [PubMed: 7644489]

Harkin LA, Bowser DN, Dibbens LM, Singh R, Phillips F, Wallace RH, Richards MC, Williams DA, Mulley JC, Berkovic SF, Scheffer IE, Petrou S. Truncation of the $GABA_A$-receptor γ2 subunit in a family with generalized epilepsy with febrile seizures plus. Am J Hum Genet. 2002; 70:530–536. [PubMed: 11748509]

Harvey K, Duguid IC, Alldred MJ, Beatty SE, Ward H, Keep NH, Lingenfelter SE, Pearce BR, Lundgren J, Owen MJ, Smart TG, Luscher B, Rees MI, Harvey RJ. The GDP-GTP exchange factor collybistin: an essential determinant of neuronal gephyrin clustering. J Neurosci. 2004; 24:5816–5826. [PubMed: 15215304]

Heron SE, Scheffer IE, Berkovic SF, Dibbens LM, Mulley JC. Channelopathies in idiopathic epilepsy. Neurotherapeutics. 2007; 4:295–304. [PubMed: 17395140]

Kalz-Füller B, Sleegers E, Schwanitz G, Schubert R. Characterisation, phenotypic manifestations and X-inactivation pattern in 14 patients with X-autosome translocations. Clin Genet. 1999; 55:362–366. [PubMed: 10422808]

Kananura C, Haug K, Sander T, Runge U, Gu W, Hallmann K, Rebstock J, Heils A, Steinlein OK. A splice-site mutation in GABRG2 associated with childhood absence epilepsy and febrile convulsions. Arch Neurol. 2002; 59:1137–1141. [PubMed: 12117362]

Kang JQ, Shen W, Macdonald RL. Why does fever trigger febrile seizures? $GABA_A$ receptor γ2 subunit mutations associated with idiopathic generalized epilepsies have temperature-dependent trafficking deficiencies. J Neurosci. 2006; 26:2590–2597. [PubMed: 16510738]

Kins S, Betz H, Kirsch J. Collybistin, a newly identified brain-specific GEF, induces submembrane clustering of gephyrin. Nat Neurosci. 2000; 3:22–29. [PubMed: 10607391]

Kneussel M, Betz H. Clustering of inhibitory neurotransmitter receptors at developing postsynaptic sites: the membrane activation model. Trends Neurosci. 2000; 23:429–435. [PubMed: 10941193]

Löw K, Crestani F, Keist R, Benke D, Brünig I, Benson JA, Fritschy JM, Rülicke T, Bluethmann H, Möhler H, Rudolph U. Molecular and neuronal substrate for the selective attenuation of anxiety. Science. 2000; 290:131–134. [PubMed: 11021797]

Maljevic S, Krampfl K, Cobilanschi J, Tilgen N, Beyer S, Weber YG, Schlesinger F, Ursu D, Melzer W, Cossette P, Bufler J, Lerche H, Heils A. A mutation in the $GABA_A$ receptor α1 subunit is associated with absence epilepsy. Ann Neurol. 2006; 59:983–987. [PubMed: 16718694]

Marco E, Abidi FE, Bristow J, Dean WB, Cotter PD, Jeremy RJ, Schwartz CE, Sherr EH. ARHGEF9 disruption in a female patient is associated with X linked mental retardation and sensory hyperarousal. J Med Genet. 2008; 45:100–105. [PubMed: 17893116]

Papadopoulos T, Korte M, Eulenburg V, Kubota H, Retiounskaia M, Harvey RJ, Harvey K, O'Sullivan GA, Laube B, Hülsmann S, Geiger JR, Betz H. Impaired GABAergic transmission and altered hippocampal synaptic plasticity in collybistin-deficient mice. EMBO J. 2007; 26:3888–3899. [PubMed: 17690689]

Rees MI, Harvey K, Pearce BR, Chung SK, Duguid IC, Thomas P, Beatty S, Graham GE, Armstrong L, Shiang R, Abbott KJ, Zuberi SM, Stephenson JB, Owen MJ, Tijssen MA, van den Maagdenberg AM, Smart TG, Supplisson S, Harvey RJ. Mutations in the human GlyT2 gene

define a presynaptic component of human startle disease. Nat Genet. 2006; 38:801–806. [PubMed: 16751771]

Schweizer C, Balsiger S, Bluethmann H, Mansuy IM, Fritschy JM, Möhler H, Lüscher B. The γ2 subunit of $GABA_A$ receptors is required for maintenance of receptors at mature synapses. Mol Cell Neurosci. 2003; 24:442–450. [PubMed: 14572465]

Shiang R, Ryan SG, Zhu YZ, Hahn AF, O'Connell P, Wasmuth JJ. Mutations in the α1 subunit of the inhibitory glycine receptor cause the dominant neurologic disorder hyperekplexia. Nat Genet. 1993; 5:351–358. [PubMed: 8298642]

Siebert PD, Chenchik A, Kellogg DE, Lukyanov KA, Lukyanov SA. An improved PCR method for walking in uncloned genomic DNA. Nucleic Acids Res. 1995; 23:1087–1088. [PubMed: 7731798]

Venkateswarlu K, Brandom KG, Lawrence JL. Centaurin-α1 is an in vivo phosphatidylinositol 3,4,5-trisphosphate-dependent GTPase-activating protein for ARF6 that is involved in actin cytoskeleton organization. J Biol Chem. 2004; 279:6205–6208. [PubMed: 14625293]

Wallace RH, Marini C, Petrou S, Harkin LA, Bowser DN, Panchal RG, Williams DA, Sutherland GR, Mulley JC, Scheffer IE, Berkovic SF. Mutant $GABA_A$ receptor γ2-subunit in childhood absence epilepsy and febrile seizures. Nat Genet. 2001; 28:49–52. [PubMed: 11326275]

Wirth J, Nothwang HG, van der Maarel S, Menzel C, Borck G, Lopez-Pajares I, Brondum-Nielsen K, Tommerup N, Bugge M, Ropers HH, Haaf T. Systematic characterisation of disease associated balanced chromosome rearrangements by FISH: cytogenetically and genetically anchored YACs identify microdeletions and candidate regions for mental retardation genes. J Med Genet. 1999; 36:271–278. [PubMed: 10227392]

Xiang S, Kim EY, Connelly JJ, Nassar N, Kirsch J, Winking J, Schwarz G, Schindelin H. The crystal structure of Cdc42 in complex with collybistin II, a gephyrin-interacting guanine nucleotide exchange factor. J Mol Biol. 2006; 359:35–46. [PubMed: 16616186]

Yee BK, Keist R, von Boehmer L, Studer R, Benke D, Hagenbuch N, Dong Y, Malenka RC, Fritschy JM, Bluethmann H, Feldon J, Möhler H, Rudolph U. A schizophrenia-related sensorimotor deficit links α3-containing $GABA_A$ receptors to a dopamine hyperfunction. Proc Natl Acad Sci USA. 2005; 102:17154–17159. [PubMed: 16284244]

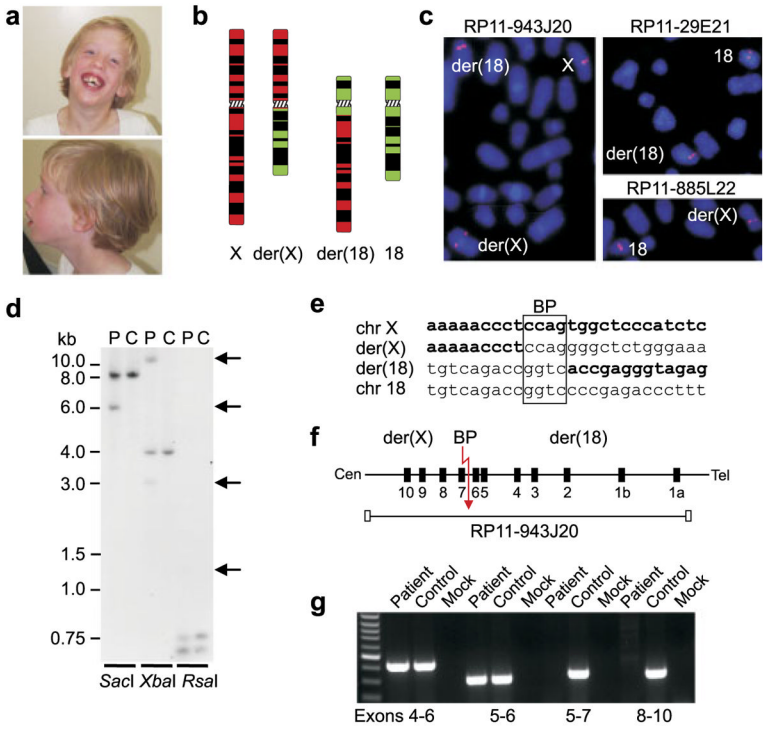

Figure 1.

Mapping a balanced chromosomal translocation in *ARHGEF9.* **A:** Patient photographs showing dysmorphic features (long and narrow face, irregular teeth, and micrognathia). **B:** Ideograms depicting the translocated chromosomes and their normal homologs. **C:** FISH analysis with chromosome 18 BAC clones with signals proximal and distal to the breakpoint and chromosome X BAC clone RP11-943J20, which spans the X breakpoint. **D:** Southern blot analysis of the breakpoint within *ARHGEF9* intron 6. *Sac*I, *Xba*I, and *Rsa*I digests revealed patient-specific bands of approximately 6, 11, 3, and 1.3 kb, which are absent in the control DNA. **E:** Sequence of the junction fragments and the respective genomic regions of the normal homologs. The four nucleotides identical in the breakpoint region and lost during rearrangement from one of the derivative chromosomes are boxed. **F:** Schematic diagram depicting *ARHGEF9* with the location of the chromosome breakpoint (arrow) as determined by FISH, breakpoint cloning, and RT-PCR experiments. The breakpoint-spanning BAC RP11-943J20 is shown below the gene. **G:** *ARHGEF9* transcript analysis in patient and control cell line RNAs. For the patient cell line, transcripts could be detected from derivative chromosome 18 (e.g., exons 4–6 and 5–6). However, no products could be obtained using primers spanning the breakpoint (exons 5–7) and within exons located proximal to the breakpoint (exons 8–10) on the derivative X chromosome. Specific bands of the expected size are present in all RT-PCRs from the control.

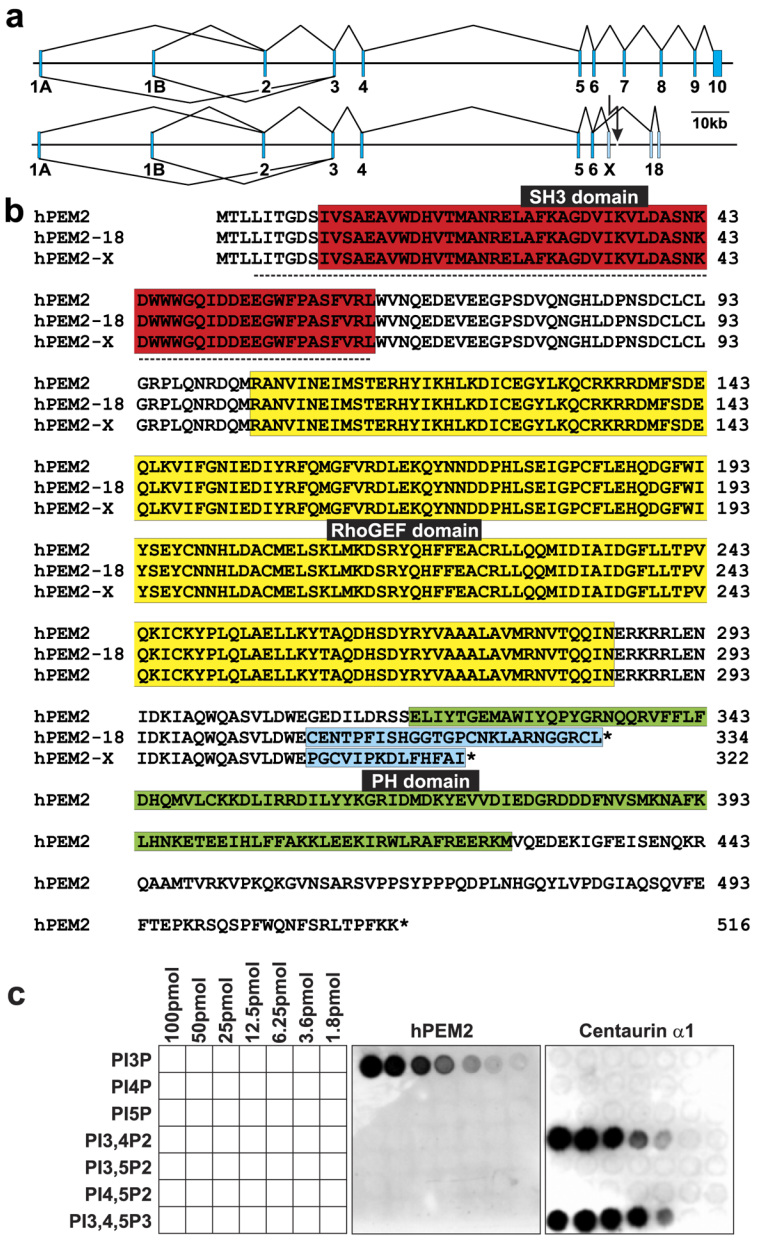

Figure 2.

Rapid amplification of cDNA ends reveals defective *ARHGEF9* transcripts resulting in a loss of the collybistin PH domain and C-terminus. **A:** Analysis of collybistin transcripts using 3′ RACE demonstrates the loss of exons 7–10 from collybistin transcripts, which are replaced by cryptic exons from chromosomes X and 18. **B:** Splicing of these cryptic exons results in the loss of the collybistin PH domain and C-terminus. **C:** Using immobilized phosphoinositides and purified GST-collybistin we found that the PH domain is functional, binding PI3P/PtdIns-3-P (phosphatidylinositol-3-phosphate) rather than PIP3/PtdIns-3,4,5-P (phosphatidylinositol 3,4,5-trisphosphate) as predicted by the “membrane activation model” of gephyrin clustering [Kneussel and Betz, 2000]. Controls using centaurin α1 verified that these overlay assays were capable of detecting binding to PIP2 and PIP3.

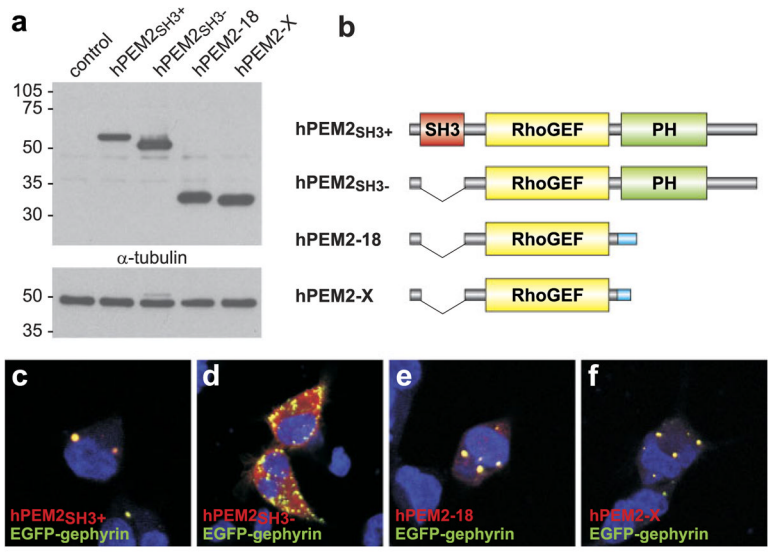

Figure 3.

Cellular models of gephyrin clustering demonstrate that hPEM2-18 and hPEM2-X colocalize with gephyrin, but do not direct the formation of submembrane microaggregates. **A:** Western blots of myc-tagged hPEM2 constructs expressed in HEK293 cells indicate that the aberrant myc-hPEM2-18 and myc-hPEM2-X proteins are stable and expressed at equivalent levels to myc-hPEM2$_{SH3+}$ and myc-hPEM2$_{SH3-}$ when compared to loading control (α-tubulin). **B:** Schematic diagram showing the domains specified by the different hPEM2 constructs. **C–F:** Coexpression of myc-tagged hPEM2 proteins with EGFP-gephyrin in HEK293 cells costained with a nuclear marker (ToPro3). As expected, myc-hPEM2$_{SH3+}$ normally colocalizes with gephyrin in large intracellular aggregates (C), while myc-hPEM2$_{SH3-}$ directs EGFP-gephyrin to submembrane clusters (D). Although they lack the regulatory SH3 domain, myc-hPEM2-18 (E) and myc-hPEM2-X (F) proteins colocalize with gephyrin, but do not direct the formation of submembrane microaggregates.

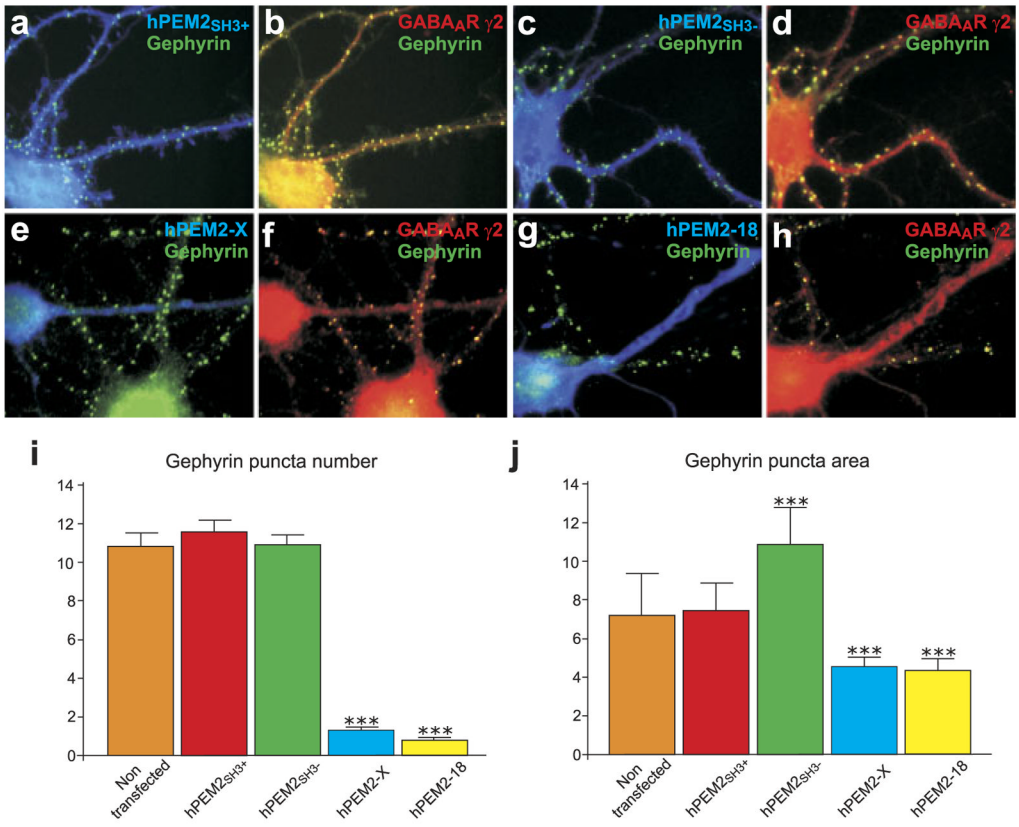

Figure 4.

Overexpression of truncated collybistin mutants in neurons results in loss of gephyrin and $GABA_AR$ clusters. Triple staining of neurons transfected with either myc-$hPEM2_{SH3+}$ (**A**,**B**), myc-$hPEM2_{SH3-}$ (**C**,**D**) or mutant constructs myc-hPEM2-X (**E**,**F**) and myc-hPEM2-18 (**G**,**H**) with antibodies against the $GABA_A$ receptor γ2 subunit (red), gephyrin (green), and myc-tag (blue). Note that myc-$hPEM2_{SH3+}$ or myc-$hPEM2_{SH3-}$ do not interfere with the colocalization of gephyrin and $GABA_A$ receptors in synaptic clusters (A–D). Quantitative analysis shows that $hPEM2_{SH3+}$ or myc-$hPEM2_{SH3-}$ do not influence gephyrin puncta number (**I**) although deletion of the regulatory SH3 domain influences puncta size (**J**). In neurons expressing myc-hPEM2-X (**E,F**) and myc-hPEM2-18 (**G,H**), gephyrin and $GABA_A$ receptor immunoreactivity is significantly reduced. Note that gephyrin and $GABA_A$ receptor clustering in neighboring neurons that do not express the myc-hPEM mutants is unaffected (**E–H**). Quantitative analysis of gephyrin immunofluorescence (**I,J**) indicates a statistically-significant loss of gephyrin clusters and a reduction in size of remaining clusters. $^{***}P<0.001$, Student's ***t***-test, n = 17–28 cells per construct.

Table 1

Phenotypic Comparison of Human *ARHGEF9* Mutations

Clinical features	Harvey et al. [2004]	Marco et al. [2008]	Present study
ARHGEF9 mutation and karyotype	p.G55A; 46,XY	46,X,inv(X)(q11.1q27.3)	46,X,t(X;18)(q11.1;q11.21)
Sex	Male	Female	Female
Age of examination	Died at age 4 years 4 months	15 years	15 years
Head circumference	Not determined	Within normal range	3rd percentile
Body height	Not determined	Within normal range	Short stature
Brain MRI	Significant brain atrophy in the cerebral cortex and cerebellar vermis	No abnormalities reported	No abnormalities reported
Mental retardation / developmental delay	Severe	Mild to moderate	Severe
Epilepsy	EEG revealed left temporal spike waves at 18 months, frequent long-lasting seizures	Not reported	First seizures at age 7 years, generalized tonic-clonic seizures
Hyperekplexia	Yes, muscle stiffness at birth and seizures provoked by tactile stimulation	Not reported	Not reported
Hyperarousal to noise	Not reported	Yes	Not reported
Behavior	Arrest and decline of psychomotor development	Autonomic hyperarousal to noise and social situations, hyperactivity, impulsivity, shyness, motor incoordination	Aggression, autoaggression, hyperactivity, frequent mood changes, disturbed sleep-wake rhythm, obstructive sleep apnea
Facial dysmorphisms	Not reported	Not reported	Long and narrow face, high narrow palate, hypertrophy of the alveolar ridge, irregular teeth, micrognathia
Other features	Not reported	Not reported	Insensitivity to thermal pain